

# Global biodiversity and the ancient carbon cycle

Daniel H. Rothman\*

Department of Earth, Atmospheric, and Planetary Sciences, Massachusetts Institute of Technology, Cambridge, MA 02139

Communicated by John M. Hayes, Woods Hole Oceanographic Institution, Woods Hole, MA, January 30, 2001 (received for review August 21, 2000)

**Paleontological data for the diversity of marine animals and land plants are shown to correlate significantly with a concurrent measure of stable carbon isotope fractionation for approximately the last 400 million years. The correlations can be deduced from the assumption that increasing plant diversity led to increasing chemical weathering of rocks and therefore an increasing flux of carbon from the atmosphere to rocks, and nutrients from the continents to the oceans. The CO<sub>2</sub> concentration dependence of photosynthetic carbon isotope fractionation then indicates that the diversification of land plants led to decreasing CO<sub>2</sub> levels, while the diversification of marine animals derived from increasing nutrient availability. Under the explicit assumption that global biodiversity grows with global biomass, the conservation of carbon shows that the long-term fluctuations of CO<sub>2</sub> levels were dominated by complementary changes in the biological and fluid reservoirs of carbon, while the much larger geological reservoir remained relatively constant in size. As a consequence, the paleontological record of biodiversity provides an indirect estimate of the fluctuations of ancient CO<sub>2</sub> levels.**

Partly as a result of the episodic nature of sedimentary processes, studies of the Earth's biologic, geologic, and climatic history have typically focused on isolated extreme events (1) such as mass extinctions (2–4) or anomalous excursions of stable chemical isotope records (5). Whereas the importance of unusual events may be nearly self-evident (6), a different, potentially powerful approach is to seek not what makes some events different from others, but that which is common to them all (7–10). In this way, one should expect to learn how fundamental invariants—for example, the conserved mass of certain chemical species—manifest themselves over geologic time.

Here we focus on biological aspects of the carbon cycle during Phanerozoic time [0–543 million years ago (Ma)]. Two types of records are studied: paleontological data for the diversity of marine animal (11) and terrestrial plant (12) life, and the sedimentary record of carbon isotope fractionation between carbon buried in organic form and carbon buried as carbonates (13). We find an unexpected significant correlation between the paleontological and geochemical records for the last 400 million years and provide evidence that it reflects the fluctuations of CO<sub>2</sub> levels in the atmosphere and oceans. Our analysis shows not only that the diversification of life appears to have depressed CO<sub>2</sub> levels (14), but also how deep this depression appears to have been.

The paper proceeds as follows. We first show the correlations of interest and subject them to several tests of statistical significance. We then discuss why CO<sub>2</sub> levels, and specific mechanisms that control them, appear to provide the link between the various records. Simple mathematical models are then formulated to clarify and quantify our arguments. Among the results is an estimate of trends in the long-term evolution of CO<sub>2</sub> levels, which we proceed to compare with previous efforts (15–19). Finally, we conclude with brief remarks on the relationship of our quantitative conclusions to their mechanistic interpretation.

## Paleontological-Geochemical Correlations

The first of two correlations is shown in Fig. 1. The data for diversity were compiled by Sepkoski<sup>†</sup> and edited by Bambach<sup>‡</sup>; they are based on the first and last geologic occurrence of 35,967 marine animal genera, including invertebrates, vertebrates, and

animal-like protists (foraminiferans and radiolarians). For each of 108 geologic stages and substages that range over Phanerozoic time, the number of genera that originate or become extinct during that stage is tabulated. If a genus passes from one (sub)stage to the next (a condition satisfied by approximately 63% of the genera), it is labeled “continuing.” The time series  $n(t)$  in Fig. 1 represents the number of continuing genera at each stage or substage boundary.

The carbon isotope record in Fig. 1 was compiled by Hayes *et al.* (13). The time series shown is obtained from measurements of the isotopic composition of organic and carbonate carbon found in sedimentary rocks formed at geologic time  $t$ . From globally averaged measurements of isotopic abundance ratios  $R_x = (^{13}\text{C}/^{12}\text{C})_x$  for carbon in sample  $x$ , the isotopic fractionation between sample  $x$  and a standard sample,  $\delta_x = 1,000[(R_x - R_{\text{STD}})/R_{\text{STD}}]$ , is obtained for carbonate ( $\delta_a$ ) and organic ( $\delta_o$ ) carbon. The isotopic fractionation  $\epsilon_{\text{toc}}$  between total organic carbon and sedimentary carbonates is then given approximately by  $\epsilon_{\text{toc}} = \delta_a - \delta_o$  (13). Fig. 1 compares  $\epsilon_{\text{toc}}(t)$  to  $n(t)$ ; the values of  $\epsilon_{\text{toc}}$ , which were obtained from global averages of thousands of independent measurements (13), are specified at 50 discrete points in time.

The two records displayed in Fig. 1 are strikingly similar after 455 Ma. Not only do both records change sharply (increasing  $n$ , decreasing  $\epsilon_{\text{toc}}$ ) at the end of the Cretaceous (65 Ma), but visually one can see that many smaller transient fluctuations are exhibited jointly. To quantify this correlation, the more finely sampled paleontological data are resampled by linear interpolation so that they are specified at the same times  $t_j$  as the geochemical data. The Spearman rank correlation coefficient  $R_s$  (25, 26) is then computed from the resulting  $N$  pairs of  $n$  and  $\epsilon_{\text{toc}}$ . We find  $R_s = -0.74$  after 455 Ma. Similar results, here and elsewhere in this paper, are obtained if “standing” diversity, the number of genera extant during a given interval, is substituted for continuing diversity.

The second correlation, shown in Fig. 2, is between the diversity of land plant families (12) and the same geochemical data. The plant data<sup>§</sup> represent standing diversity at the family level in 67 geologic stages since the rise of land plants in the Silurian (425 Ma). From the late Devonian (370 Ma) onwards, the correlation between the two records is essentially the same as that found in Fig. 1:  $R_s = -0.77$ .

We use three different methods to assess the statistical significance  $P$  of these correlations. The results are summarized in Table 1. For completeness, we report results for the entire available interval in addition to the slightly shorter periods cited

Abbreviation: Ma, million years ago.

See commentary on page 4290.

\*E-mail: dan@segovia.mit.edu.

<sup>†</sup>J. J. Sepkoski, Spring 1996 version of the genus-level database that appeared in an earlier form in ref. 11.

<sup>‡</sup>R. K. Bambach, personal communication. The original Sepkoski dataset was timed according to Harland *et al.* (20), with changes to the Cambrian following Bowring *et al.* (21). Bambach's updates include retiming of the Cenozoic (22), placing the Permian–Triassic boundary at 251 Ma (23), and the Permian–Carboniferous boundary at 301 Ma (24).

<sup>§</sup>The compilation is available on the Internet at <http://palaeo.gly.bris.ac.uk/frw/whole/fr2.html>.

The publication costs of this article were defrayed in part by page charge payment. This article must therefore be hereby marked “advertisement” in accordance with 18 U.S.C. §1734 solely to indicate this fact.

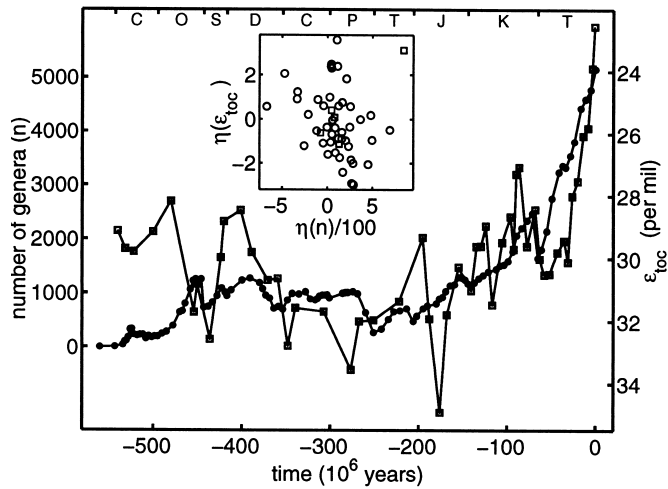


**Fig. 1.** Phanerozoic fluctuations of diversity  $n(t)$ , the number of marine animal genera (filled circles) (11), and  $\varepsilon_{\text{toc}}(t)$ , the isotopic fractionation between inorganic and organic carbon [open squares, in per mil] (13). The vertical axis for  $\varepsilon_{\text{toc}}$  increases downward. The data track each other reasonably well after 455 Ma. Sample standard deviations for the geochemical data range from 0.3 to 2.9‰, averaging 1.5‰ before the Cretaceous (144 Ma) and 0.9‰ afterwards (13). Rough error bars for diversity may be inferred from ref. 11. The time scale for  $\varepsilon_{\text{toc}}$  has been revised (slightly) from the original to match the updated scheme used for diversity. The capital letters (except for K) correspond to the following geologic periods: Cambrian, Ordovician, Silurian, Devonian, Carboniferous, Permian, Triassic, Jurassic, Cretaceous, and Tertiary. (Inset) The whitened sequence  $\eta_j(\varepsilon_{\text{toc}})$  vs.  $\eta_j(n)$  obtained by prediction-error filtering. Squares and circles represent data before and after 455 Ma, respectively.

above. We argue later that only the latter periods are relevant to our conclusions.

In the first method, a Monte Carlo technique, we construct random realizations of each time series that satisfy the autocorrelations of the original data. Denoting either the diversity or  $\varepsilon_{\text{toc}}$  data as  $x_j = x(t_j)$ , the method proceeds by Fourier transforming  $x$  [after multiplying by a Hanning window (26) and removing the mean] to obtain  $N$  complex Fourier coefficients  $\hat{x}_k$ . Random time series  $x_j^f$  are then generated by computing the inverse Fourier transform such that  $x_j^f = \sum_k |\hat{x}_k| e^{i(\phi_k + 2\pi jk/N)}$ , where  $\phi_k$  is uniformly distributed between  $-\pi$  and  $\pi$  while satisfying the symmetries required for  $x_j^f$  to be real.  $P$  values are then estimated by computing the fraction of  $10^6$  simulated time-series pairs that yield rank correlation coefficients  $R_s$  less than those obtained for the actual data.<sup>†</sup>

The second method applies a first-order prediction-error filter (27) to each time series. In principle, this converts the time series to white noise, thereby eliminating the additional variance of the estimated correlation coefficient caused by significant autocorrelation of  $x_j$  at nonzero lags (28). Denoting the white-noise sequence by  $\eta_j = x_j + ax_{j-1}$ , we choose  $a$  by minimizing the sum of the squared forward and backward prediction error,  $\sum_{j=2}^N (\tilde{x}_j + a\tilde{x}_{j-1})^2 + (\tilde{x}_{j-1} + a\tilde{x}_j)^2$ , where  $\tilde{x}_j = x_j - N^{-1}\sum_{j=1}^N x_j$ . We obtain  $a = -0.98$  for both diversity series and  $a = -0.73$  for  $\varepsilon_{\text{toc}}$ . The rank correlation coefficient between  $\eta_j(n)$  and  $\eta_j(\varepsilon_{\text{toc}})$  is then computed, along with the associated one-sided statistical significance  $P$  obtained from Student's  $t$ -distribution with  $N - 3$  degrees of freedom. The *Insets* in Figs. 1 and 2 show plots of  $\eta_j(n)$  vs.  $\eta_j(\varepsilon_{\text{toc}})$ .

<sup>†</sup>Because the theory constructed later requires the assumption that diversity and  $\varepsilon_{\text{toc}}$  are negatively correlated, we test specifically for the probability  $P$  that a negative correlation with magnitude at least as great as that observed could be obtained under the null hypothesis that diversity and  $\varepsilon_{\text{toc}}$  are uncorrelated.

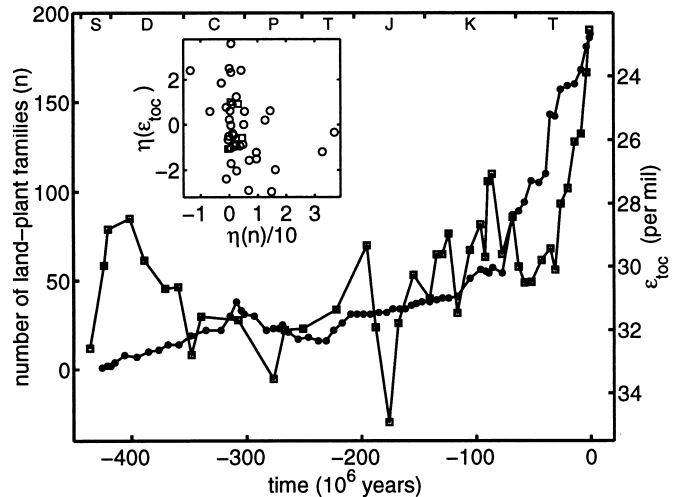


**Fig. 2.** The diversity  $n$  of terrestrial plant families (filled circles) (12) plotted with the same geochemical data (open squares) of Fig. 1, beginning with the rise of land plants in the Silurian (425 Ma). The vertical axis for  $\varepsilon_{\text{toc}}$  again increases downward. The data track each other reasonably well after 370 Ma. The geologic time scale is the same as in Fig. 1. The diversity curve shown is the “minimal” curve of the plant family database; rough error bars may be inferred by comparison with the corresponding “maximal” curve. (Inset) The whitened sequence  $\eta_j(\varepsilon_{\text{toc}})$  vs.  $\eta_j(n)$  obtained by prediction-error filtering. Squares and circles represent data before and after 370 Ma, respectively.

The third method, included as a reference, constructs  $\eta_j$  by computing serial differences, i.e., by setting  $a = -1$  above. This is equivalent to assuming that all three time series are realizations of a random walk.

Table 1 shows that all three methods find that the negative correlations quoted above are statistically significant, usually with  $P < 0.01$ . The Monte Carlo method typically yields the lowest  $P$  values, whereas serial differencing yields the highest. Because the former method requires the fewest assumptions and the latter the most, it seems reasonable to associate the greatest credence with the Monte Carlo results.

### Decomposition of the Geochemical Signal

To understand why the paleontological and geochemical data correlate negatively, consider the following decomposition of  $\varepsilon_{\text{toc}}$  (13):

$$\varepsilon_{\text{toc}} = \varepsilon_p + \Delta_{\text{carb}} - \Delta_2. \quad [1]$$

Here  $\varepsilon_p$  represents the isotopic effects of primary production (i.e., photosynthesis),  $\Delta_{\text{carb}}$  is the isotopic depletion of dissolved  $\text{CO}_2$  in surface waters relative to sedimentary carbonate, and  $\Delta_2$  represents isotopic shifts caused by the reworking of organic carbon before burial. The quantity  $\Delta_{\text{carb}}$  depends mainly on surface water temperature and ranges from about 7 per mil (‰) at  $30^\circ\text{C}$  to  $10\text{‰}$  at  $3^\circ\text{C}$  (13); this  $3\text{‰}$  range is much less than the  $12\text{‰}$  range of  $\varepsilon_{\text{toc}}$ . The secondary processes symbolized by  $\Delta_2$  are defined such that  $\Delta_2$  is positive when the process enriches the  $^{13}\text{C}$  content of organic matter. One of the principal components of  $\Delta_2$  derives from the structure of food webs: the  $^{13}\text{C}$  content of many animals is enriched by approximately  $1\text{‰}$  relative to its food (29–31). Thus as diversity grows, one might naively expect the size of food webs and therefore the length of food chains to grow, and thus also  $\Delta_2$ , thereby explaining the negative correlation of  $\varepsilon_{\text{toc}}$  with  $n$ . However, contemporary food chains nearly always contain about four trophic levels, and this length depends so weakly on the size of the food webs within which the chains are embedded (32) that it appears unlikely that food chains are

**Table 1. Spearman rank correlation coefficients  $R_s$  from correlations of  $\varepsilon_{\text{toc}}$  with the diversity of marine animal genera and land plant families**

Data	$R_s$	$P$	$N$	$R_s$	$P$	$N$
Marine animals		After 540 Ma			After 455 Ma	
Raw	-0.52	0.084	50	-0.74	$<10^{-3}$	45
PEF	-0.32	0.013	49	-0.40	0.003	44
Differences	-0.20	0.087	49	-0.28	0.035	44
Land plants		After 425 Ma			After 370 Ma	
Raw	-0.58	0.026	42	-0.77	$<10^{-4}$	38
PEF	-0.37	0.010	41	-0.40	0.007	37
Differences	-0.26	0.052	41	-0.29	0.041	37

In each case, correlations are computed three ways: by using the raw data, by correlating the output of a prediction-error filter (PEF) computed for each time series, and by correlating serial differences. Results are shown for the entire available intervals and also subsets formed by deleting the first few data points. The one-sided statistical significance  $P$  is computed by a Monte Carlo technique for the raw data and from Student's  $t$ -distribution in the other cases.

responsible for the correlation. Moreover, the net effect of all secondary biological processes is such that even the *sign* of  $\Delta_2$  is debated (31), and recent estimates put  $\Delta_2$  at the relatively small and constant value of 1.5‰ throughout the Phanerozoic (13). In summary, the combined fluctuations of  $\Delta_{\text{carb}}$  and  $\Delta_2$  should amount to no more than about 3‰, which is less than one-fourth of the variation of  $\varepsilon_{\text{toc}}$  during the Phanerozoic.

The photosynthetic processes represented by  $\varepsilon_p$  (13, 31, 33, 34) thus encode the only plausible explanations for the bulk of the  $\varepsilon_{\text{toc}}$ 's variations. Recent research indicates that plankton photosynthesis produces an isotopic shift in  $^{13}\text{C}$  content that may be approximated by the empirical relation (34)

$$\varepsilon_p = \varepsilon_f - \frac{\mu v_s}{\kappa[\text{CO}_2]}, \quad [2]$$

where  $\varepsilon_f \approx 25\text{--}30\text{‰}$  (35) is the isotopic shift associated with carbon fixation,  $\kappa$  is proportional to the permeability of the algal cell wall,  $v_s$  is the volume-to-surface-area ratio of the cell,  $\mu$  is the specific growth rate, and  $[\text{CO}_2]$  is the concentration of dissolved carbon dioxide. The isotopic enrichment  $\varepsilon_f$  derives primarily from the kinetic discrimination against  $^{13}\text{C}$  by the enzyme Rubisco in the Calvin-Benson or photosynthetic carbon reduction cycle. It may be expected to have remained approximately constant in marine environments since the first appearance of eukaryotes at least two billion years ago (35). However, the physiological parameters  $\kappa$ ,  $v_s$ , and  $\mu$  can vary significantly across phytoplankton species (33, 34). Along with  $[\text{CO}_2]$ , they control the relative rate at which  $\text{CO}_2$  diffuses into the algal cell compared to the rate at which  $\text{CO}_2$  is consumed by photosynthetic reactions within the cell. Whereas the long-term evolution of  $[\text{CO}_2]$  should be independent of these parameters, they may have evolved in response to changes in  $[\text{CO}_2]$ . For example, decreases in  $[\text{CO}_2]$  could have led to increases in cell permeabilities  $\kappa$  such that the diffusive flux of  $\text{CO}_2$  into the algal cell was relatively unchanged. Provided that such evolutionary innovations are not fully compensating—i.e., so long as  $\kappa[\text{CO}_2]$  increases with  $[\text{CO}_2]$ —then the correlations between diversity and  $\varepsilon_{\text{toc}}$  should reflect correlations between diversity and  $[\text{CO}_2]$ . More generally, this conclusion remains valid for any dependence of the physiological parameters on  $[\text{CO}_2]$ , provided that  $\mu v_s/(\kappa[\text{CO}_2])$  decreases with increasing  $[\text{CO}_2]$  and no direct relationship between the physiological parameters and diversity exists.

### Mechanisms and Dynamics

Unlike the short-term carbon cycle, which is dominated by exchanges of carbon between the biosphere, atmosphere, oceans, and soils on time scales ranging from about  $10^0\text{--}10^4$  years, the long-term carbon cycle is dominated by exchanges

between rocks and the atmosphere and oceans on time scales of roughly  $10^5\text{--}10^9$  years (14–16, 36, 37). Three slow processes dominate the long-term evolution of  $\text{CO}_2$  levels: chemical weathering of silicate minerals, degassing caused by metamorphic and volcanic processes, and the burial and weathering of organic carbon. Because the latter acts as an independent subcycle (14), the former—weathering and degassing—are considered the major controls on atmospheric and oceanic  $\text{CO}_2$  levels. They are thought to be in rough balance via reactions such as (14, 36, 38)



A similar reaction may be written by substituting Mg for Ca. Left to right, such reactions schematically represent the uptake of  $\text{CO}_2$  from the atmosphere, its transformation to dissolved  $\text{HCO}_3^-$  during weathering of silicate rocks, and its eventual precipitation and burial in the oceans as carbonate minerals. Right to left, the reaction represents metamorphism and magmatism and the subsequent transfer of  $\text{CO}_2$  back to the atmosphere and oceans by volcanism and related processes.

The mechanistic basis of our observed correlations is simple: increased plant diversity should result in increased chemical weathering of silicate minerals. We assume, following others (14–18, 39), that the increased chemical and physical alterations of soils—e.g., the mechanical breakdown of rocks and the production of organic acids—induced by the advent of vascular land plants should have led to substantial increases in weathering rates. This notion is augmented with two assumptions: (i) increased plant diversity increases the area occupied by plants (by, for example, migration of plants to higher altitudes), therefore enhancing weathering rates and lowering  $\text{CO}_2$  levels via Eq. 3; and (ii) increased weathering increases the seaward flux of limiting nutrients such as phosphorus, which in turn leads to increased marine animal diversity. The former assumption is sufficient to explain the correlation between land plant diversity and  $\varepsilon_{\text{toc}}$ , whereas the latter is also required to explain the correlation with the marine ecosystem. Both of these assumptions may be subsumed in part by the simpler supposition that global diversity increases with global productivity or biomass, a point we return to below.

To complete our argument, we must show not only that increased plant diversity can lead to lower  $\text{CO}_2$  levels, but also that the lower  $\text{CO}_2$  levels are dynamically stable. The rate of uptake of  $\text{CO}_2$  by the weathering reactions should increase with the partial pressure of atmospheric  $\text{CO}_2$ , which at long time scales should be an increasing function of the total mass  $m_f$  of carbon in the Earth's fluid envelope (i.e., atmospheric and oceanic carbon) (14). We represent the bare uptake rate, in the absence of plants, by the positive monotonically increasing function  $k(m_f)$  while representing the return flux of  $\text{CO}_2$ , from volcanic and other sources, by  $v$  [which should not depend on  $m_f$

EVOLUTION

GEOLOGY

(14)]. All other processes aside, the rate of change of the mass of atmospheric and oceanic carbon is then

$$\dot{m}_f = v - k(m_f)g(n), \quad [4]$$

where  $g(n) \geq 1$  is a monotonically increasing function that represents the ratio of the CO<sub>2</sub> uptake rate when plant diversity equals  $n$  to the bare uptake rate  $k$ .

The steady state  $m_f^*$  of this system occurs when  $\dot{m}_f = 0$ ; thus

$$m_f^* = k^{-1}[v/g(n)], \quad [5]$$

where  $k^{-1}$  is the inverse of  $k$  such that  $k^{-1}[k(x)] = x$ . Because  $k^{-1}$  must also be a monotonically increasing function, Eq. 5 shows that increasing plant diversity  $n$  causes the steady-state mass of atmospheric and oceanic carbon,  $m_f^*$ , to decrease. The steady state is stable if  $d\dot{m}_f/dm_f < 0$  when  $m_f = m_f^*$ . From Eq. 4, one finds that  $m_f^*$  is indeed stable, because

$$d\dot{m}_f/dm_f = -g(n)dk/dm_f < 0 \quad [6]$$

for any  $m_f$ . This result follows immediately by noting that  $dk/dm_f > 0$  and  $g(n) \geq 1$ .

A complete representation of the long-term carbon cycle is of course vastly more complex (14–16, 36). The model expressed by Eq. 4 does, however, serve to formalize our main point: if increasing plant diversity increases weathering rates, then CO<sub>2</sub> levels fall. We proceed to quantify by how much.

### Relative Fluctuations of Carbon Reservoirs

We consider the mass of three reservoirs of carbon: the fluid reservoir, already denoted by  $m_f$ , the biological reservoir  $m_b$  (i.e., biomass plus biological debris), and the geological reservoir  $m_g$  (i.e., rocks). Present-day estimates give  $m_b \approx 10^{-1}m_f \approx 10^{-5}m_g$  (35, 37).

In globally averaged steady-state conditions, [CO<sub>2</sub>] increases with  $m_f$  (40). The inverse relationship is likewise increasing, i.e.,

$$m_f = h_f([\text{CO}_2]), \quad [7]$$

where  $h_f$  is a monotonically increasing function.

A monotonic relationship probably also exists between diversity and  $m_b$ . Waide *et al.* (41) have recently compiled a comprehensive review of over 200 published relationships between present-day diversity and primary productivity, where primary productivity is broadly defined to include various surrogates, such as biomass, that vary positively with it. One of the few unambiguous patterns to emerge from their survey is the dependence of the diversity–productivity relationship on scale. Whereas at local scales (<20 km) simple relationships (positive, negative, or unimodal) are usually not found [or when they are, they are often unimodal (42)], at continental to global scales (>4,000 km), a positive correlation dominates the literature, particularly for plants. Additional evidence of such scale dependence is given in ref. 43, and examples of unambiguously positive large-scale relationships may be found in ref. 44. The positive large-scale relation may derive from the tendency of ecosystems to diversify when more energy is available for consumption (45). Similar relationships appear to hold for the past: Bambach (46) cites a wealth of evidence indicating that the biomass of marine animals has trended upward during the Phanerozoic. Thus it appears reasonable to assume that the mass  $m_b$  of the biological reservoir of carbon increases with diversity  $n$ , i.e.,

$$m_b = h_b(n), \quad [8]$$

where  $h_b$  is monotonically increasing. The assumption that increased diversity is associated with increased weathering rates may be viewed as a natural consequence of this relationship.

We may now relate the correlations between  $n$  and  $\varepsilon_{\text{toc}}$  to  $m_b$  and  $m_f$ . First, rewrite Eq. 2 as

$$\varepsilon_{\text{toc}} = \varepsilon_0 - \gamma/[\text{CO}_2], \quad [9]$$

where  $\gamma = \mu\nu_s/\kappa$  represents the physiological parameters appropriately averaged over all phytoplankton species, and

$$\varepsilon_0 = \varepsilon_f - \Delta_2 + \Delta_{\text{carb}}. \quad [10]$$

Now assume that  $\varepsilon_0$  is constant and  $\gamma/[\text{CO}_2]$  decreases with increasing [CO<sub>2</sub>]. In the former case, the only time dependence should come from  $\Delta_{\text{carb}}$ , and as we have already remarked, its mean-square fluctuations must be much smaller than those of  $\gamma/[\text{CO}_2]$ . Thus this assumption appears reasonable. The latter assumption is satisfied automatically if  $\gamma$  is constant. The less stringent condition used here derives from the aforementioned evolutionary considerations, i.e.,  $\gamma$  can change, but never so much that it fully compensates (or overcompensates) changes in [CO<sub>2</sub>].

Let  $R_l(x, y)$  and  $R_s(x, y)$  be the functions that compute the linear [product-moment (25)] and rank correlation coefficients, respectively, between discretely sampled time series  $x(t)$  and  $y(t)$ . Because  $R_s$  is a correlation of ranks, it is invariant with respect to any monotonically increasing transformation of its arguments (25). From Table 1 and Eqs. 7, 8, and 9, we have

$$0 > R_s(n, \varepsilon_{\text{toc}}) = R_s(n, \varepsilon_0 - \gamma/[\text{CO}_2]) \quad [11]$$

$$= R_s(n, -[\text{CO}_2]^{-1}) \quad [12]$$

$$= R_s(n, [\text{CO}_2]) \quad [13]$$

$$= R_s(m_b, m_f). \quad [14]$$

These results derive from the invariance property of  $R_s$ , the condition that [CO<sub>2</sub>] > 0, and the assumptions that  $\varepsilon_0$  is constant,  $\gamma/[\text{CO}_2]$  decreases with increasing [CO<sub>2</sub>], and  $\gamma$  is uncorrelated with  $n$ . The final equality shows that the mass fluctuations of the biological and fluid reservoirs of carbon are negatively correlated, with the same magnitude as found for diversity and  $\varepsilon_{\text{toc}}$ .

This conclusion may be sharpened. In the following, we assume that any measurable coupling between  $m_b$  and  $m_f$  requires  $m_b$  to be sufficiently large, as a consequence of sufficient diversification on land. We therefore explicitly consider only the period after 370 Ma, when both marine animals and land plants exhibit their strongest correlations to  $\varepsilon_{\text{toc}}$ .

Because the Earth's total carbon is conserved,

$$m_b + m_f + m_g = \text{const}. \quad [15]$$

The fluctuations  $\tilde{m}_i = m_i - \langle m_i \rangle$ , where  $\langle \cdot \rangle$  signifies the mean over the entire interval, satisfy

$$\tilde{m}_b + \tilde{m}_f = -\tilde{m}_g. \quad [16]$$

Squaring both sides, rearranging terms, and averaging over time, one obtains

$$2\langle \tilde{m}_b \tilde{m}_f \rangle = \langle \tilde{m}_g^2 \rangle - \langle \tilde{m}_b^2 \rangle - \langle \tilde{m}_f^2 \rangle. \quad [17]$$

We seek the sign of  $\langle \tilde{m}_b \tilde{m}_f \rangle$ . Mathematically, it must have the same sign as the linear correlation coefficient  $R_l(m_b, m_f)$ .  $R_l$  and its variance may be estimated from  $R_s$  under the assumption that  $\tilde{m}_b$  and  $\tilde{m}_f$  are Gaussian. We use the relations  $R_l = 2 \sin(\pi R_s/6)$  and  $\text{var } R_l = (\pi^2/9)(1 - R_l^2/4) \text{var } R_s$  (25). Substituting  $R_s = -0.40$  from Table 1 (i.e., the estimate obtained by prediction–error filtering) and an estimate of  $\text{var } R_s$  obtained by the bootstrap method (47) (averaged for both marine animals and land plants), we find  $R_l = -0.42 \pm 0.13$  (one standard deviation). Consequently,  $\langle \tilde{m}_b \tilde{m}_f \rangle < 0$  with high probability, and therefore, on substitution into Eq. 17,

$$\langle \tilde{m}_g^2 \rangle < \langle \tilde{m}_b^2 \rangle + \langle \tilde{m}_f^2 \rangle. \quad [18]$$

This inequality, which we have obtained here for the long-term million-year time scale, is an important counterintuitive result. It shows that the mean-square fluctuations of the geologic reservoir are less than those of the biological and fluid reservoirs combined—despite the fact that rocks contain nearly all the Earth’s carbon! The long-term depletion of  $m_f$  is therefore not only due to the growth of  $m_b$ , but most of  $m_f$ ’s fluctuations are complementary (i.e., of opposite sign) to  $m_b$ ’s. Consequently, an estimate of the changes of either quantity provides an estimate of the changes of the other.

### Estimate of Past CO<sub>2</sub> Levels

We define the dimensionless CO<sub>2</sub> concentration  $\phi = [\text{CO}_2]_{\varepsilon_0}/\gamma$  and substitute into Eq. 9 to obtain

$$\phi(t) = \frac{\varepsilon_0}{\varepsilon_0 - \varepsilon_{\text{loc}}(t)}. \quad [19]$$

In this formulation, the physiological parameters subsumed into  $\gamma$  no longer appear. We are obliged, however, to choose a value for  $\varepsilon_0$ . In the following,  $\varepsilon_0$  ranges from 36‰ to 38‰, which is consistent with the known variations of its constituents.

Rather than obtaining  $\phi$  directly from Eq. 19, we estimate it indirectly from a combination of the geochemical and diversity data of Fig. 1. We fit the estimate of  $\phi$  obtained from Eq. 19 to a linear model for  $\phi(n)$ :

$$\phi = \phi_0 - bn. \quad [20]$$

In this model,  $\phi_0$  is the dimensionless CO<sub>2</sub> concentration before the diversification of animals and land plants, whereas the second term represents the first-order effect of increasing diversity. For  $\varepsilon_0 = 38‰$ , we find  $\phi_0 = 6.6 \pm 0.4$  and  $b = (8.0 \pm 1.7) \times 10^{-4}$  by linear regression.

Given estimates of  $\phi_0$  and  $b$ , we then estimate  $\phi(t)$  itself by setting  $n = n(t)$  in Eq. 20. The result, normalized by  $\phi(0)$ , is shown in Fig. 3 for the cases  $\varepsilon_0 = 36‰$  and  $\varepsilon_0 = 38‰$ . Fig. 3 also shows a comparison with analogous predictions from the numerical model of Berner (15–18). Berner’s model is a detailed integration of estimated carbon fluxes caused by chemical weathering, volcanic degassing, and carbon burial; the uncertainty of his estimates is qualitatively reflected by the gray area in Fig. 3.

Comparison of the results from our model with Berner’s shows that the pattern of decreasing CO<sub>2</sub> levels since ~225 Ma is roughly equivalent in both. This trend is also qualitatively consistent with estimates based on the carbon isotopic composition of paleosols (48–51), plant stomatal ratios (52), carbon isotopic measurements from marine sediments (53), and an alternative reconstruction based on estimates of the Earth’s inventory of buried carbon (19). However, the period before 225 Ma shows distinct differences from Berner’s predictions. Although our estimate falls within Berner’s region of uncertainty, it shows relatively no change compared to Berner’s steep decrease at ~300 Ma. Moreover, recent estimates from paleosols (54, 55) and plant stomatal ratios (52) are in accord with this dip. If the dip is indeed real, the mismatch with our model would presumably be caused by missing ingredients, such as changes in the burial rate of organic carbon accompanied by compensatory changes in algal cell permeabilities.

### Conclusion

Surprising correlations exist between paleontological records of biodiversity and the carbon isotope fractionation evident in

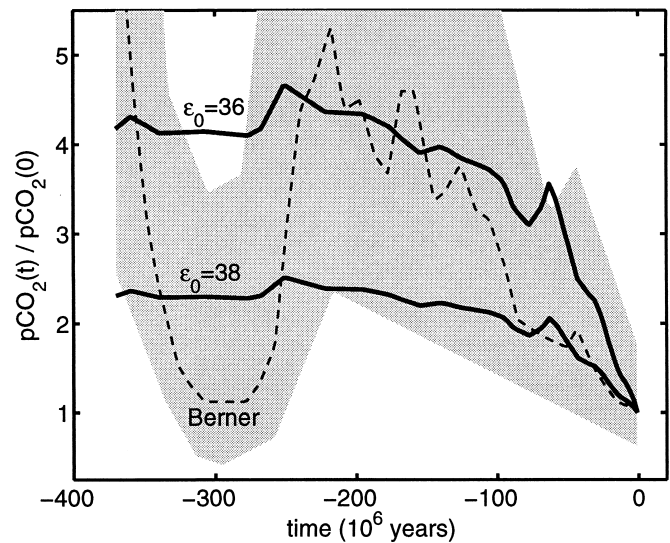


**Fig. 3.** Smooth curves: estimates of the normalized partial pressure of atmospheric CO<sub>2</sub> [ $p\text{CO}_2$ , which is proportional to  $[\text{CO}_2]$  (40)] for the last 370 million years, obtained from the model Eq. 20 and the least-squares estimates of the parameters  $\phi_0$  and  $b$ , for the cases  $\varepsilon_0 = 36‰$  and  $\varepsilon_0 = 38‰$ . Because Eq. 20 is linear in  $n$ , these curves are simply the diversity curve of Fig. 1 upside down and rescaled. Dashed curve and gray area: prediction from the model of Berner (15, 16) and its region of qualitative uncertainty, respectively, from ref. 17.

the sedimentary record for the last 370 million years. Proceeding from the assumptions that (i) chemical weathering rates grow with plant diversity; (ii) diversity grows with biomass at the global scale; and (iii) changes in phytoplankton physiology neither correlate with diversity nor fully compensate changes in CO<sub>2</sub> levels, we find that the correlations express complementary fluctuations in the size of the organic and inorganic carbon reservoirs within the biosphere, atmosphere, and hydrosphere. Consequently, CO<sub>2</sub> levels decreased as biodiversity increased. These conclusions imply that fluctuations of CO<sub>2</sub> levels have been driven primarily by changes within the biosphere and only secondarily by purely geologic and geophysical processes. However, such a causal relationship is not required for our principal quantitative conclusions—the Inequality 18 and the downward trend in Fig. 3—to hold. Indeed, our analysis leaves open the possibility, for example, that tectonically induced reductions of CO<sub>2</sub> levels led to increased diversity in both continental and marine ecosystems. A definitive statement of causation will require further work that includes not only the study of other geochemical signals (10) but also improved paleontological records.

I thank A. Knoll for introducing me to the study of Earth history, A. Knoll and R. Bambach for access to the late Jack Sepkoski’s unpublished genus-level database, and R. Bambach for his generous technical assistance with the paleontological data. I also thank J. Hayes, not only for access to his data before publication, but also for clarifying many of the finer points of carbon-isotope geochemistry. Finally, I thank S. Bowring, E. Boyle, P. Dodds, J. Edmond, B. Enquist, D. Erwin, H. Hartman, C. Marshall, D. Raup, N. Schorghofer, and J. Weitz for helpful discussions. This work was supported in part by National Science Foundation Grant DEB-0083983.

1. Walliser, O. H., ed. (1996) *Global Events and Event Stratigraphy in the Phanerozoic* (Springer, Berlin).
2. Erwin, D. H. (1993) *The Great Paleozoic Crisis: Life and Death in the Permian* (Columbia Univ. Press, New York).
3. Kemp, T. S. (1999) *Fossils and Evolution* (Oxford Univ. Press, Oxford, U.K.).

4. Courtillot, V. (1999) *Evolutionary Catastrophes* (Cambridge Univ. Press, New York).
5. Hoffman, P. F., Kaufman, A. J., Halverson, G. P. & Schrag, D. P. (1998) *Science* **281**, 1342–1346.
6. Alvarez, L. W., Alvarez, W., Asaro, F. & Michel, W. V. (1980) *Science* **208**, 1095–1108.

7. Fischer, A. G. (1984) in *Catastrophes and Earth History: The New Uniformitarianism*, eds. Berggren, W. A. & Van Couvering, J. A. (Princeton Univ. Press, Princeton, NJ), pp. 129–150.
8. Raup, D. M. & Sepkoski, J. J. (1984) *Proc. Natl. Acad. Sci. USA* **81**, 801–805.
9. Worsley, T. R., Nance, D. & Moody, J. B. (1984) *Mar. Geol.* **58**, 373–400.
10. Veizer, J., Ala, D., Azmy, D., Bruckschen, P., Buhl, D., Bruhn, F., Carden, G., Diener, A., Ebner, S., Godderis, Y., et al. (1999) *Chem. Geol.* **161**, 59–88.
11. Sepkoski, J. J. (1996) in *Global Events and Event Stratigraphy*, ed. Walliser, O. H. (Springer, Berlin), pp. 35–52.
12. Benton, M. J., ed. (1993) *The Fossil Record 2* (Chapman & Hall, London).
13. Hayes, J. M., Strauss, H. & Kaufman, A. J. (1999) *Chem. Geol.* **161**, 103–125.
14. Walker, J. C. G. (1977) *Evolution of the Atmosphere* (Macmillan, New York).
15. Berner, R. A. (1991) *Am. J. Sci.* **291**, 339–376.
16. Berner, R. A. (1994) *Am. J. Sci.* **294**, 56–91.
17. Berner, R. A. (1997) *Science* **276**, 544–546.
18. Berner, R. A. (1998) *Philos. Trans. R. Soc. London Ser. B* **353**, 75–82.
19. Budyko, M. I., Ronov, A. B. & Yanshin, A. L. (1987) *History of the Earth's Atmosphere* (Springer, Berlin).
20. Harland, W. B., Armstrong, R., Cox, A., Craig, L., Smith, A. G. & Smith, D. G. (1990) *A Geologic Time Scale 1989* (Cambridge Univ. Press, Cambridge, U.K.).
21. Bowring, S. A., Grotzinger, J. P., Isachsen, C. E., Knoll, A. H., Pelchaty, S. M. & Kolosov, P. (1993) *Science* **261**, 1293–1298.
22. Berggren, W. A., Kent, D. V., Swisher, C. C., III & Aubry, M.-P. (1995) in *Geochronology, Time Scales, and Global Stratigraphic Correlation*, eds. Berggren, W. A., Kent, D. V., Aubry, M.-P. & Hardenbol, J. (Society for Sedimentary Geology, Tulsa, OK) No. 54, pp. 129–212.
23. Bowring, S. A., Erwin, D. H., Jin, Y. G., Martin, M. W., Davidek, K. & Wang, W. (1998) *Science* **280**, 1039–1045.
24. Rasbury, E. T., Hanson, G. N., Meyers, W. J., Holt, W. E., Goldstein, R. H. & Saller, A. H. (1998) *Geology* **26**, 403–406.
25. Kendall, M. G. & Gibbons, J. D. (1990) *Rank Correlation Methods*. (Oxford Univ. Press, New York), 5th Ed.
26. Press, W. H., Flannery, B. P., Teukolsky, S. A. & Vetterling, W. T. (1995) *Numerical Recipes in C: The Art of Scientific Computing* (Cambridge Univ. Press, Cambridge, U.K.).
27. Claerbout, J. F. (1976) *Fundamentals of Geophysical Data Processing* (McGraw-Hill, New York).
28. Box, G., Jenkins, G. M. & Reinsel, G. C. (1994) *Time Series Analysis: Forecasting and Control* (Prentice-Hall, Upper Saddle River, NJ), 3rd Ed.
29. DeNiro, M. J. & Epstein, S. (1978) *Geochim. Cosmochim. Acta* **42**, 495–506.
30. McConnaughey, T. & McRoy, C. P. (1979) *Mar. Biol.* **53**, 257–262.
31. Hayes, J. M. (1993) *Mar. Geol.* **113**, 111–125.
32. Cohen, J. E., Briand, F. & Newman, C. M. (1990) *Community Food Webs* (Springer, Berlin).
33. Rau, G. H., Riebesell, U. & Wolf-Gladrow, D. (1997) *Global Biogeochem. Cycles* **11**, 267–278.
34. Popp, B. N., Laws, E. A., Bidigare, R. R., Dore, J. E., Hanson, K. L. & Wakeham, S. G. (1998) *Geochim. Cosmochim. Acta* **62**, 69–77.
35. Falkowski, P. G. & Raven, J. A. (1997) *Aquatic Photosynthesis* (Blackwell Science, Malden, MA).
36. Holland, H. D. (1978) *The Chemistry of the Atmosphere and Oceans* (Wiley, New York).
37. Des Marais, D. J. (1997) in *Geomicrobiology: Interactions Between Microbes and Minerals*, eds. Banfield, J. F. & Nealson, K. H. (Mineralogical Soc. Am., Washington, DC), pp. 429–448.
38. Urey, H. C. (1952) *The Planets* (Yale Univ. Press, New Haven, CT).
39. Algeo, T. J. & Scheckler, S. E. (1998) *Philos. Trans. R. Soc. London Ser. B* **353**, 113–130.
40. Broecker, W. S. & Peng, T.-H. (1982) *Tracers in the Sea* (Lamont-Doherty Geological Observatory, Palisades, NY).
41. Waide, R. B., Willig, M. R., Steiner, C. F., Mittelbach, G., Gough, L., Dodson, S. I., Juday, G. P. & Parmenter, R. (1999) *Annu. Rev. Ecol. Syst.* **30**, 257–300.
42. Rosenzweig, M. L. (1995) *Species Diversity in Space and Time* (Cambridge Univ. Press, Cambridge, U.K.).
43. Wright, D. H., Currie, D. J. & Maurer, B. A. (1993) in *Species Diversity in Ecological Communities*, eds. Ricklefs, R. E. & Schluter, D. (Univ. of Chicago Press, Chicago, IL), pp. 66–74.
44. Currie, D. J. (1991) *Am. Nat.* **137**, 27–49.
45. Wright, D. H. (1983) *Oikos* **41**, 496–506.
46. Bambach, R. K. (1993) *Paleobiology* **19**, 372–397.
47. Efron, B. & Tibshirani, R. J. (1993) *An Introduction to the Bootstrap* (Chapman & Hall, New York).
48. Cerling, T. E. (1991) *Am. J. Sci.* **291**, 377–400.
49. Sinha, A. & Stott, L. D. (1994) *Global Planet. Change* **9**, 297–307.
50. Andrews, J. E., Tandon, S. K. & Dennis, P. F. (1995) *J. Geol. Soc. (London)* **152**, 1–3.
51. Ghosh, P., Bhattacharya, S. K. & Jani, R. A. (1995) *Palaeogeogr. Palaeoclimatol. Palaeoecol.* **114**, 285–296.
52. McElwain, J. C. (1998) *Philos. Trans. R. Soc. London Ser. B* **353**, 83–96.
53. Freeman, K. & Hayes, J. M. (1992) *Global Biogeochem. Cycles* **6**, 185–198.
54. Mora, C. I., Driese, S. G. & Colarusso, L. A. (1996) *Science* **271**, 1105–1107.
55. Yapp, C. J. & Poths, H. (1996) *Earth Planet. Sci. Lett.* **137**, 71–82.